A Novel Approach for Imaging of Thoracic Outlet Syndrome Using Contrast-Enhanced Magnetic Resonance Angiography (CE-MRA), Short Inversion Time Inversion Recovery Sampling Perfection with Application-Optimized Contrasts Using Different Flip Angle Evolutions (T2-STIR-SPACE), and Volumetric Interpolated Breath-Hold Examination (VIBE)

Authors' Contribution:
Study Design A
Data Collection B
Statistical Analysis C
Data Interpretation D
Manuscript Preparation E
Literature Search F
Funds Collection G

ABCDEFG 1 Tonghua Zhang
B 1 Zhengdao Xu
B 1 Jianxin Chen
BG 2 Zongbao Liu
A 3 Tao Wang
B 1 Yijiang Hu
B 1 Liping Shen
B 1 Feifei Xue

1 Department of Radiology, Zhangjiagang Hospital Affiliated to Soochow University, Suzhou, Jiangsu, P.R. China
2 Department of Orthopedics, Zhangjiagang Hospital Affiliated to Soochow University, Suzhou, Jiangsu, P.R. China
3 Department of Hand Surgery and Shanghai Key Laboratory of Peripheral Nerve and Microsurgery, Fudan University Huashan Hospital, Shanghai, P.R. China

Corresponding Author: Zongbao Liu, e-mail: liuzongbao1102@163.com
Source of support: This study was supported by the Zhangjiagang Technology Bureau (ZKS1729) and Shanghai Key Laboratory of Peripheral Nerve and Microsurgery (17DZ2270500)

Background: The aim of this study was to introduce a novel method combining contrast-enhanced magnetic resonance angiography (CE-MRA), short inversion time inversion recovery sampling perfection with application-optimized contrasts using different flip angle evolutions (T2-STIR-SPACE) and volumetric interpolated breath-hold examination (VIBE) sequences in the assessment of thoracic outlet syndrome (TOS).

Material/Methods: CE-MRA, T2-STIR-SPACE, and VIBE techniques were employed to evaluate neurovascular bundles in 27 patients clinically suspected of TOS. Images were evaluated to determine the cause of neurovascular bundle compression. Surgical exploration was performed in patients with abnormal magnetic resonance imaging (MRI) results.

Results: Twenty patients were found to be abnormal: 6 cases showed only neurogenic TOS and the correlates included infraclavicular hemangiomas (n=1) and transverse cervical artery (n=5). Arterial-neurogenic TOS was found in 4 cases, including subclavian lymph node metastasis from breast cancer (n=3) and schwannoma (n=1). Arterial-venous-neurogenic TOS was found in 1 subject, and the correlates included a fibrous band from the cervical rib and elongated C7 transverse process. In this case, the subclavian artery/vein was compressed dynamically. Venous–neurogenic TOS was noted in one subject. Nine patients were considered as post-traumatic TOS, including brachial plexus edema (n=3), the brachial plexus rupture (n=2), peri-brachial plexus effusion (n=3), and stenosis of the SCA (n=1). In the remaining 7 patients, MRI did not detect abnormalities.

Conclusions: TOS can be evaluated by CE-MRA, T2-STIR-SPACE, and VIBE during a single examination, with a reduced contrast material dose. This imaging modality performs well in showing the anatomical structure of the neurovascular bundle and the cause of the compression.

MeSH Keywords: Brachial Plexus • Magnetic Resonance Imaging • Nerve Compression Syndromes • Thoracic Outlet Syndrome

Full-text PDF: https://www.medscimonit.com/abstract/index/idArt/919358

📄 1855   📊 1   📈 3   📚 25

Background

Thoracic outlet syndrome (TOS) is caused by abnormal compression of the brachial plexus and/or subclavian artery/vein (neurovascular bundle) as they traverse the thoracic outlet [1]. TOS can be classified as vascular or neural diseases, or both, depending on the compromise to specific structures in the cervico-axillary canal [2]. The neurovascular compression due to many different causes.

The diagnosis of TOS is usually accomplished by careful medical history, physical examination (irritant examination), radiological examination, and electrodiagnostic examination. Imaging examination is helpful for diagnosis. However, because of the complex structure of the thoracic outlet, imaging is a challenge.

In most cases, plain film examinations are used to detect skeletal abnormalities. Contrast-enhanced CT is used to detect bone and vascular structures. Catheterography is another invasive technique for the diagnosis of vascular TOS.

Ultrasound imaging can detect vascular pathologies and may also be applied to NTOS [3,4]. This technique, however, is limited by skeletal coverage and obesity [5], and requires more rigorous evaluation [6]. These methods are difficult to repeat and perform poorly in demonstrating the neurovascular bundles, accessory muscles, or fibrous bands. This information is important because the purpose of treating thoracic outlet symptoms is to alleviate or reduce compression in narrow spaces. Contrast-enhanced MRA and equilibrium phase are useful in this process [7]. Post-contrast 3D-T2-STIR is another tool used in assessing the brachial plexus [8].

To establish a reliable noninvasive imaging method to demonstrate the neurovascular bundle, localize the site of compression, the compressing structure, and the compressed vessel or mass among patients with suspected TOS, a new technique involving CE-MRA, 3D T2-STIR-SPACE, and 3D-VIBE was used to assess neurovascular bundle with a single contrast injection. We successfully assessed 27 consecutive cases on a standard 1.5T magnetic resonance scanner within 10 min, with excellent visualization of the nerve and vascular bundles at the thoracic outlet.

Material and Methods

Patients

This study was approved by the local Human Experiment and Ethics Committee. Written informed consent was obtained from each participant. A total of 27 patients (9 men and 18 women) with a mean age of 44.8±14.7 years were studied. The inclusion criterion was clinical suspicion of TOS. Symptoms included arm pain, paresthesia, numbness, muscle weakness, heaviness, ischemic changes, edema, arm fatigue, ulcers, and gangrene. The physical examination results were normal, except that in 6 patients raising the hands over the head caused symptoms to appear (n=6). Underlying injuries resulted from sports injuries, motor vehicle crashes, and factory accidents (n=9). Three patients suffered from clavicular fractures and 1 was diagnosed as soft tissue injury of the neck or shoulder.

Image acquisition

All imaging was performed on a 1.5-T Avanto MRI scanner (Siemens, Erlangen, Germany) from June 2014 to December 2018. The combination of the body coil and neck coil was used to improve signal reception. Gadopentetate dimeglumine (Magnevist Bayer HealthCare) was used as a contrast agent. An intravenous catheter was placed on the patient's upper extremity on the asymptomatic side.

The pulse sequence and imaging parameters of the protocol used by our organization are summarized in Table 1. Sequences were programmed as follows: First, breath-hold arterial phase contrast-enhanced MR angiography (CE-MRA) covering from the aortic arch to the distal radial artery with arms alongside the body was acquired. An automated power bolus injector was used for administration of 15 ml of contrast medium and 20 ml of saline at a rate of 3 ml/s. Then, the coronal post-contrast isotropic 3D T2-STIR-SPACE sequence was performed. The scan range was from the anterior vertebral body to the posterior vertebral body, including both sides of the brachial plexus. Last, a coronal 3D volumetric interpolated breath-hold examination (3D VIBE) was performed.

Table 1. The set of sequences used for MRI investigation of the thoracic outlet.

Sequence	Orientation	FOV (mm)	Slice thickness (mm)	TR/TE (ms)	Voxel size
3D contrast-enhanced MRA	Coronal	320	0.85	3.49/1.32	0.8×0.8×0.8
3D VIBE	Coronal	300	1.2	7.33/2.39	1.2×1.2×1.2
3D STIR SPACE	Coronal	360	1.2	3800/350	1.2×1.2×1.2
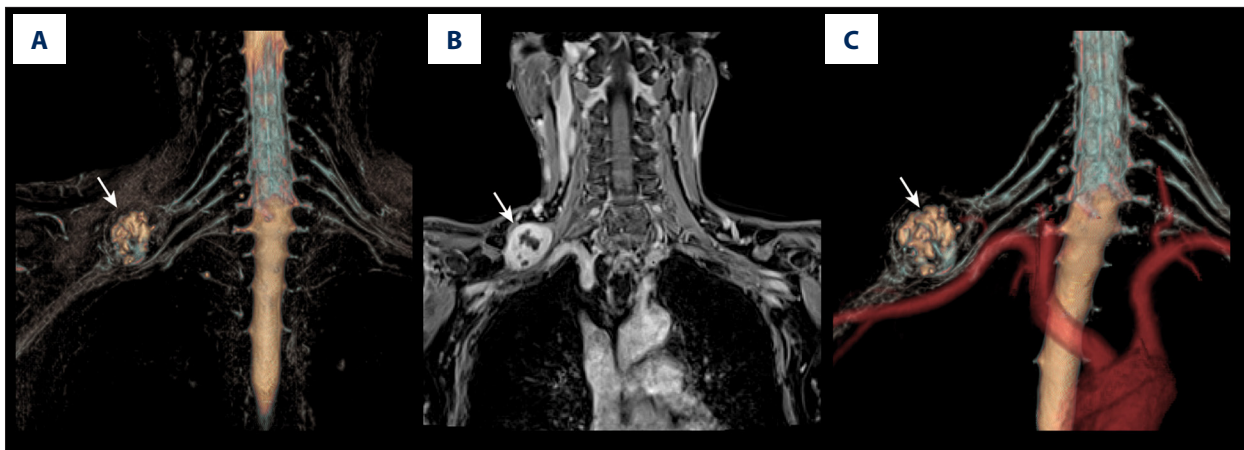
Figure 1. Pathologically proven schwannoma of brachial plexus in a 40-year-old patient with right arm dysesthesia. (**A**) 3D T2-STIR-SPACE volume rending (VR) image of the brachial plexus revealed a round mass (arrow) in the upper trunk. (**B**) The tumors showed inhomogeneous contrast enhancement on the venous phase coronal VIBE image (arrows head). (**C**) 3D-synchro-view demonstrates the relationship of the mass to the surrounding vessels, and the subclavian artery was compressed and displaced (arrow).

Six of the examinations were repeated with the same approaches with the arms extended overhead, which was specifically requested by the clinicians [9].

Image interpretation

All images were evaluated on a 3D workstation (GE Advantage Workstation, GE Healthcare, Milwaukee, WI, USA) in a consensus manner by 2 radiologists blinded to clinical symptoms. Radiologists are allowed to use source images to obtain any or all of the available post-processing image reconstruction algorithms, including 2D and 3D maximum intensity projection (MIP), multiplanar reconstruction (MPR), cross-section analysis, 3D synchro-view, and volume-rendered image.

Since previous publications reported a correlation between neurovascular compression and bone abnormalities in 90% of cases [10–12], we first reviewed chest X-rays to determine if there were anatomical abnormalities (such as cervical spine fractures or cervical ribs). Then, we evaluated the potential compression of the brachial plexus by adjacent structures and the signal changes of T2W indicative of nerve damage.

In the evaluation of vessels, the source image and maximum intensity projection were retrospectively reviewed and assessed for significant persistent stenosis or impingement. The relationship of the vessels to the brachial plexus was analyzed by 3-dimensional synchro-view.

The positive imaging findings were then confirmed by the diagnostic criterion standard of surgery, and the cause of the impingement was then removed. Symptoms were significantly improved in all surgical patients.

Results

All subjects completed the study. Seven of the 27 patients were normal and 20 of the 27 patients were found to be abnormal. In the normal neurovascular bundles, 5 cases were related to cervical spondylosis and 2 cases were associated with median and ulnar nerve injuries related to the patients' symptoms.

Among the abnormal-appearing neurovascular bundles, 6 cases showed only neurogenic TOS, and the correlates included infraclavicular hemangiomas (n=1) and transverse cervical artery (n=5).

Four patients had arterial-neurogenic TOS due to subclavian lymph node metastasis – from breast cancer in 3 patients and from schwannoma in 1 patient (Figure 1).

Arterial-venous-neurogenic TOS was noted in 1 subject; cervical rib and elongated C7 transverse process were found on plain radiographs in this patient. 3D T2-STIR-SPACE sequence showed the brachial plexus was compressed by hypointense fibrous bands. The subclavian artery/vein was compressed by the clavicle when the affected arm elevated, which resolved at rest (Figure 2).

In 1 subject, venous-neurogenic TOS was noted, and the compression was due to a hematoma (Figure 3).

Nine patients were considered as post-traumatic TOS. The brachial plexus edema was detected within the compressed plexus portion due to clavicular fractures (n=3) or the roots or trunks of the brachial plexus rupture (n=2). The peri-brachial plexus effusion was detected in 3 patients (n=3). CE-MRA revealed persistent moderate stenosis of the SCA in only 1 patient.
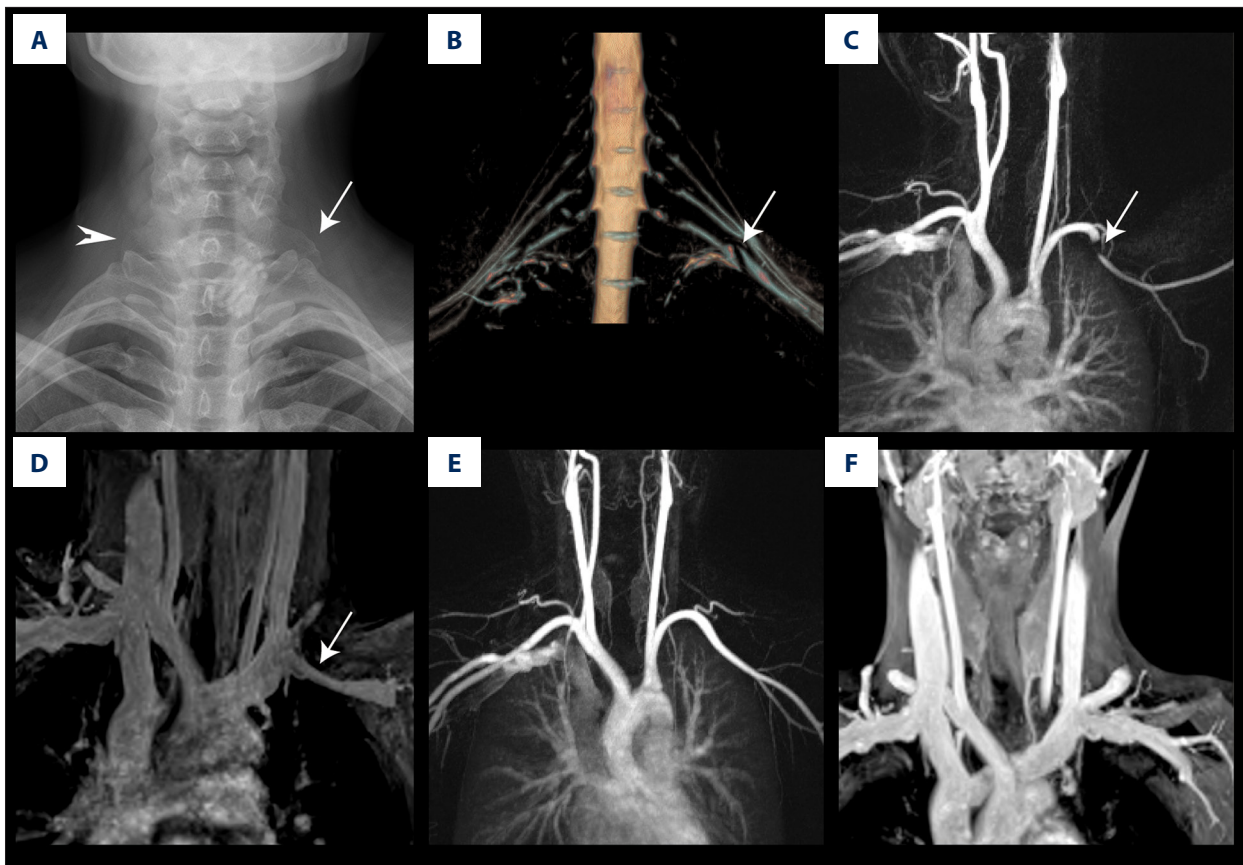
Figure 2. A 40-year-old patient with left arm pain and Adson test showed loss of radial pulse with arm abduction. (**A**) Plain radiograph shows an elongated C7 transverse process on the right (arrowhead) and an incomplete cervical rib on the left (arrow); (**B**) 3D-T2-STIR SPACE clearly shows the impingement of the brachial plexus by hypointense fibrous bands; (**C**) CE-MRA with the arms abducted shows significant compression in the mid-left subclavian artery (arrows). (**D**) Venous phase VIBE image coronal maximum-intensity-projection (MIP) image shows significant compression of left SCV (arrow) at the costoclavicular region during arm abduction. (**E**) A coronal MIP image of arterial phase MRA during armrest shows the resolution of stenosis. (**F**) Venous phase VIBE image coronal maximum-intensity-projection (MIP) image shows resolution of left SCV compression during arm rest.

Discussion

In the present study, we introduced a CE-MRA, VIBE, and 3D-T2-STIR SPACE sequence to demonstrate the neurovascular structures and to identify causes of neurovascular compression in the thoracic outlet. We found this method is useful to demonstrate the brachial plexus and the subclavian artery/vein (neurovascular bundle) situated between the clavicle and the first thoracic rib, as well as to localize the site of compression, the compressing structure, and the compressed vessel or mass among patients with suspected TOS.

The subclavian artery/vein can be assessed by MR angiography and post-contrast 3D-VIBE. CE-MRA has been explored and proven to be helpful for the diagnosis of vascular TOS [13]. Arterial TOS is most often associated with the cervical or abnormal first rib [14]. In our TOS cases, 5 subjects displayed

compression of both the brachial plexus and the subclavian artery. We were able to evaluate the subclavian vein in all patients because contrast-enhanced 3D-VIBE can better characterize veins and more reliably diagnose venous stenosis or thrombosis. In our study population, we encountered 1 case of significant venous stenosis. Contrast-enhanced 3D-VIBE also helps identify other chest pathological abnormalities, such as external masses that compress neurovascular structures.

Post-contrast 3D-STIR SPACE after CE-MRA can significantly suppress background signals, improving contrast for better delineation of the brachial plexus. It is useful for displaying tumors and compression of the brachial plexus [15]. In our study, contrast-enhanced 3D-T2-STIR SPACE sequence was helpful in the visualization of the brachial plexus and soft tissue masses within the thoracic inlet owing to suppressing background signals of surrounding tissues and paraspinal vessels. STIR SPACE
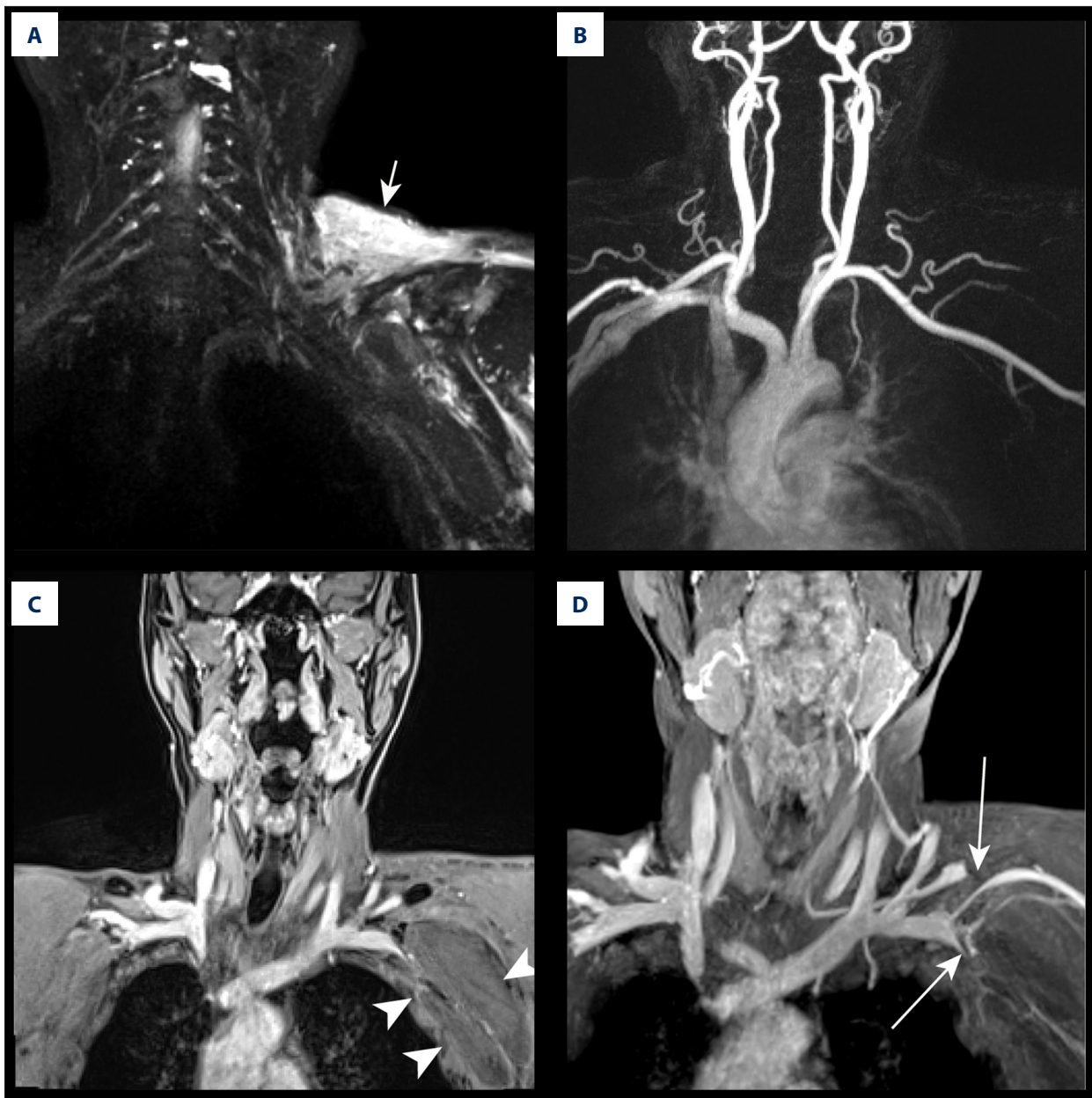
Figure 3. A 72-year-old man with left arm swelling and finger numbness after shoulder trauma. (**A**) 3D-T2-STIR SPACE shows compression of left brachial plexus and wide-spread soft tissue edema of the left shoulder (arrow). (**B**) Contrast-enhanced MR angiography shows the left subclavian artery was normal. (**C**) Venous phase coronal VIBE image revealed a large axillary hematoma (arrows head). (**D**) Venous phase VIBE maximum-intensity-projection (MIP) image shows significant compression (arrows) of left subclavian veins (SCVs) and suprascapular vein.

can be used to assess congenital fibromuscular abnormalities and their relationship to neurovascular bundles. Chest radiographs can demonstrate bony abnormalities. In our study, 3D-T2-STIR SPACE provided other useful information beyond the plain radiograph. A sharp fibrous band was shown by 3D-T2- STIR SPACE, which was verified during surgery. Fibrous bands as compressive structures were reported by Thomas and Cushing in 1903 and has since been observed regularly

in situ by anatomists and surgeons [16–19].In addition to the described anatomy of the compressed brachial plexus, T2W abnormality within the affected nerves and peri-brachial plexus effusion was also observed on STIR SPACE.

The postural factor was regarded as the underlying pathology of non-specific TOS. Postural abnormalities are attributed to muscle imbalance caused by hypertrophy or atrophy of

various muscle groups [20–22]. In our study, 6 of the examinations were performed with the arms extended overhead, which was specifically requested by the clinicians. Linear compression of the subclavian artery was shown with arms raised, which resolved in 2 subjects with the arms down. Thus, MRI sequences with the arms raised can be useful in the assessment of dynamic compression of vessels.

Traumatic neurovascular TOS is a common disorder that most often results from mid-clavicular fractures [23,24]. The blood vessels or the brachial plexus located between the clavicle and the first thoracic rib are injured secondarily [25]. In our study, clavicular fracture and brachial plexus injury coexisted in the majority of cases.

In our study, MR did not detect abnormalities in 7 patients with clinically suspected TOS. Five patients were associated with cervical spondylosis, which explained the patient's symptoms, rather than as a type of TOS. Two patients were associated with median and ulnar nerve injuries demonstrated using electromyography.

In our study group, many patients had mixed causes. This imaging modality could classify thoracic outlet syndrome into neurogenic, arterial, venous, or mixed causes during a single examination. Thus, the contrast material dose can be decreased.

This imaging approach has some advantages over other noninvasive imaging modalities. In our study population, vascular and neurologic compression could be observed together. However, 3D CE-MRA, contrast-enhanced equilibrium phase imaging, and T2-weighted pulse sequence alone can only define the type of TOS as arterial TOS, venous TOS, or neurogenic TOS separately. Moreover, the patients with clinical suspicion of TOS can be evaluated by our imaging approach during 1 examination with a reduced contrast material dose.

There are some limitations to our study. First, bone abnormalities can be difficult to identify at MR imaging but are best identified on plain radiograph. Second, gadolinium is a contrast agent that is toxic to people with kidney and liver disease. MRA cannot be performed in patients with low glomerular filtration rate. Third, we did not investigate the differences in findings of magnetic resonance imaging (MRI) at neutral and provocative locations. Lastly, our patients had various causes of brachial plexus diseases. Further prospective studies are recommended in future work to focus on certain types of brachial plexus neuropathy.

Conclusions

For evaluation of patients with clinical suspicion of TOS, combined CE-MRA, 3D T2-STIR-SPACE, and 3D-VIBE is feasible during a single examination, can inform the clinician about the exact cause and precise sites of the compression, and is also useful for surgical intervention planning.

Conflict of interest

None.

References:

1. Lafosse L, Gupta A, Lafosse T et al: Nerve entrapment syndromes in the shoulder, brachial plexus, and thoracic outlet syndrome in athletes. Sports Injuries, 2015; 425–37

2. Lawrence C, Tosti RJ: Anatomy of the ulnar nerve and cubital tunnel. Cubital Tunnel Syndrome. Springer, Cham, 2019; 3–13

3. Longley D, Yedlicka JW, Molina E et al: Color Doppler ultrasound of thoracic outlet syndrome. Seminars in interventional radiology. Thieme Medical Publishers, Inc. 1990; 7(03/04): 230–35

4. Leonhard V, Smith R, Caldwell G et al: Anatomical variations in the brachial plexus roots: Implications for diagnosis of neurogenic thoracic outlet syndrome. Ann Anat, 2016; 206: 21–26

5. Ghouri MA, Gupta N, Bhat AP et al: CT and MR imaging of the upper extremity vasculature: Pearls, pitfalls, and challenges. Cardiovasc Diagn Ther, 2019; 9(Suppl. 1): S152–73

6. Povlsen S, Povlsen B: Diagnosing thoracic outlet syndrome: Current approaches and future directions. Diagnostics (Bael), 2018; 8(1): pii: E21

7. Aghayev A, Rybicki FJ: State-of-the-art magnetic resonance imaging in vascular thoracic outlet syndrome. Magn Reson Imaging Clin N Am, 2015; 23(2): 309–20

8. Zhang X, Li M, Guan J et al: Evaluation of the sacral nerve plexus in pelvic endometriosis by three-dimensional MR neurography. J Magn Reson Imaging, 2017; 45(4): 1225–31

9. Illig KA, Donahue D, Duncan A et al: Reporting standards of the Society for Vascular Surgery for thoracic outlet syndrome. J Vasc Surg, 2016; 64(3): e23–35

10. Hussain MA, Aljabri B, Al-Omran M: Vascular thoracic outlet syndrome[C]// Seminars in thoracic and cardiovascular surgery. WB Saunders, 2016; 28(1): 151–57

11. Gelabert HA, Rigberg DA: Thoracic outlet syndrome and vascular disease of the upper extremity. Moore's Vascular and Endovascular Surgery E-Book: A Comprehensive Review, 2018; 479

12. Wells FC, Coonar AS: Excision of first rib for thoracic outlet syndrome. Thoracic surgical techniques. Springer, Cham, 2018; 69–72

13. Thakor AS, Chung J, Patel P et al: Use of blood pool agents with steady-state MRI to assess the vascular system. J Magn Reson Imaging, 2017; 45(6): 1559–72

14. Kuhn JE, Lebus GF, Bible JE: Thoracic outlet syndrome. J Am Acad Orthop Surg, 2015; 23(4): 222–32

15. Vargas MI, Gariani J, Delattre BA et al: Three-dimensional MR imaging of the brachial plexus. Seminars in musculoskeletal radiology. Thieme Medical Publishers, 2015; 19(02): 137–48

16. Arányi Z, Csillik A, Böhm J et al: Ultrasonographic identification of fibromuscular bands associated with neurogenic thoracic outlet syndrome: The "wedge-sickle" sign. Ultrasound Med Biol, 2016; 42(10): 2357–66

17. Lafosse T, Le Hanneur M, Lafosse L: All-endoscopic brachial plexus complete neurolysis for idiopathic neurogenic thoracic outlet syndrome: A prospective case series. Arthroscopy, 2017; 33(8): 1449–57

18. Lavergne P, Khuong HT: Neurogenic thoracic outlet syndrome. Peripheral Nerve Neurosurgery, 2018; 71

19. Hussain MA, Aljabri B, Al-Omran M: Vascular thoracic outlet syndrome. Seminars in thoracic and cardiovascular surgery. WB Saunders, 2016; 28(1): 151–57

20. Leonhard V, Smith R, Caldwell G et al: Anatomical variations in the brachial plexus roots: implications for diagnosis of neurogenic thoracic outlet syndrome. Ann Anat, 2016; 206: 21–26

21. Badri H, Bhattacharya V: Diagnosis and management of thoracic outlet syndrome. Postgraduate Vascular Surgery: A Candidate's Guide to the FRCS and Board Exams. 2018

22. Stogicza A, Singh V, Trescot A: Neurogenic thoracic outlet syndrome. Pain Management: A Problem-Based Learning Approach, 2018; 53

23. Ashman BD, Tewari A, Castle J et al: Intraoperative neuromonitoring for brachial plexus neurolysis during delayed fixation of a clavicular fracture presenting as thoracic outlet syndrome: A case report. JBJS Case Connect, 2018; 8(4): e85

24. Gieger J, Beers F, Birrer K et al: Misalignment of the clavicle after intramedullary fixation of a midshaft fracture with a titanium elastic nail results in acute neurovascular thoracic outlet syndrome. J Shoulder Elbow Surg, 2016; 25(4): e110–14

25. Kluemper C, Koestner T, Cowart J et al: Intercostal entrapment of clavicle fracture causing a pulseless, flaccid upper extremity. J Hand Surg Am, 2018; 43(12): 1143.e1–1143.e4.